

## Response to Anonymous Reviewer #1

The authors are grateful to the anonymous reviewer for carefully reading the manuscript and the proposed corrections. Accordingly to the comments following changes were made:

**1)** *In Introduction, it is difficult to comprehend notations with regards to particles and model coordinates.*

First paragraph in Introduction (beginning from the line 17, page 1 up to the line 8, page 2) was reformulated as follows:

The relationship between the near-surface flux  $F_s(x, y, 0)$  and the flux  $F_s(x_M, y_M, z_M)$ , measured in point  $\mathbf{x}_M = (x_M, y_M, z_M)$ , can be formalized via the footprint function  $f_s$ :

$$F_s(x_M, y_M, z_M) = \int_{-\infty}^{\infty} \int_{-\infty}^{\infty} f_s(x, y, x_M, y_M, z_M) F_s(x, y, 0) dx dy. \quad (1)$$

Traditionally, footprint functions  $f_s^d(x^d, y^d, \mathbf{x}_M) = f_s(x, y, \mathbf{x}_M)$  are expressed in local coordinate system with the origin which coincides with the sensor position (here,  $x^d = x_M - x$  is the positive upwind distance from the sensor and  $y^d = y_M - y$  is the cross-wind distance, see Fig. 1a). In horizontally homogenous case these functions do not depend on  $x_M$  and  $y_M$ . In ABL the surface area contributing to the flux is elongated in wind direction, therefore the cross-wind integrated footprint function  $f_s^y$  defined as

$$f_s^y(x^d, z_M) = \int_{-\infty}^{\infty} f_s^d(x^d, y^d, z_M) dy^d, \quad (2)$$

is one of the most required characteristics for the practical use.

The measurements of the scalar flux footprint functions in natural environment are restricted (e.g., Finn et al., 1996; Leclerc et al., 1997, 2003; Nicolini et al., 2015) due to the necessity to conduct the emission and detection of artificial tracers. Besides, such measurements are not available for the stably stratified ABL where the area of the surface influencing the point of measurements increases.

Here we avoided introducing of the averaging notations, which bring no additional sense in original version of manuscript. Systems of coordinates are illustrated in additional schematic Fig. 1a.

**2)** *A new figure would help to explain the analysis and experiment set up. E.g. it is*

unclear why  $\mathbf{x}_M$  is a vector but  $x, y$  not in Eq. (1). It is hard to understand what the coordinates of particles are and how the weight areas are computed. The figure should refer to Eq. (1) (2) and (3) and to the description on the page 4 lines 20-35..

New schematic figure was added (Fig.1). It was supplemented with the appropriate description of footprint evaluation algorithm in Section 2.1:

Schematic representation of the algorithm for the footprint function determination in LES is shown in Fig. 1. In accordance with Eq. (3) and the description above, the particle crossing the test area  $\delta_M$  brings the impact into the value  $f_s(x_S, y_S, \mathbf{x}_M)$  then the beginning of its modified trajectory shifted in a such way to superpose the point  $\mathbf{x}_1^p$  with sensor position  $\mathbf{x}_M$  belongs to the test area  $\delta_S$ . For example (see, Fig. 1b), red particle is counted while evaluation of the footprint value in point  $(x_S, y_S)$ , but blue particle is not counted. Such algorithm of averaging was selected because it permits to refine the footprint resolution in the vicinity of sensor independently on the area of  $\delta_M$  using the assumption of some spatial homogeneity.

Besides, we added description of the grid used for footprint accumulation (see last paragraph of Sect. 2.1 in modified version of manuscript):

Nonuniform Cartesian grid  $\mathbf{x}_{ij}^d = (x_i^d, y_j^d)$  (where,  $-20 \leq i \leq 160$ ;  $-120 \leq j \leq 120$ ), stretched with the distance from the sensor position, was selected for the footprint functions accumulation in the following sections of this paper. Grid was prescribed as:  $(x_0^d, y_0^d) = (0, 0)$ ;  $x_i^d = \Delta_{x0} \gamma_x^{|i|} i / |i|$  and  $y_j^d = \Delta_{y0} \gamma_y^{|j|} j / |j|$  if  $i \neq 0$  and  $j \neq 0$ ;  $\Delta_{x0} = \Delta_{y0} = 2$  m;  $\gamma_x = \gamma_y = 1.05$ . This grid is independent on the LES model resolution and coincides with the footprint grids selected for all runs with LSMs and RDMs.

**3) Explain what "ensemble average" means in the context of the study.**

The following clarification was included after the Eq. (8) in Sect. 2.3:

Here  $\langle u_i^{(p)} \rangle$  is the ensemble averaged Eulerian velocity at point  $\mathbf{x}^p$ . Note, that LSMs are assumed to be also applicable under the temporal evolution of turbulence statistics. In this paper we shall consider ABL as it approaches a quasi-steady state. Therefore, due to assumption of er-

godicity, ensemble averaging can be replaced by averaging in time and in the directions of spatial homogeneity:  $\langle \varphi \rangle \approx \langle \varphi \rangle_{x,y,t}$ .

**3)** *Why is the index "p" used both as subscript and superscript in Eq. (7) and later on. Could you make notations more homogeneous?*

The notation  $s_p$  was used to denote evaluated value of scalar concentration by the number of particles (subscript  $p$  was not connected with the superscript  $p$ ). In new version of manuscript we denote this value  $s_P$  (with capital  $P$ ) to avoid misunderstanding.

**5)** *Page 6, lines 2-3. The sentence is not quite clear. What will happen if a particle leaves the volume and then reappears again in the same volume during the unit time interval? Will it be counted as a new particle? Or do you mean something different under "appearing ... during unit time interval".*

The word "appearing" was replaced by word "ejected". Here we mean the new particles which were added during the run (appearing of new particles imitates the external source of scalar concentration).

**6)** *The sentence between Eqs. (8) and (9) is impossible to understand.*

This sentence was rewritten as follows:

Single particle first-order LSM is formulated as follows. Velocity  $u_i^p$  is described by the stochastic differential equation: ...

**7)** *Page 9, line 25. Use "provides better agreement" instead of "leads to better coincidence".*

It was done.

**8)** *Section 4.2.3, also 5.1.4 and 5.1.5. It would be useful to place a discussion here into some experimental context referring to correlations between resolved and unresolved*

*velocities (or velocities and stresses on different spatial scales) , e.g. the work by Charles Meneveau and co-authors (Meneveau and Katz in Annu. Rev. Fluid Mech. 2000. 32:1–32).*

The paper (Meneveau and Katz, 2000) is devoted to the a priori testing of the scale-similarity approaches for subgrid modelling of Eulerian dynamics in LES. The reference to this paper is useful in Section 3.1 where the mixed subgrid/subfilter model is introduced. So, the following text was added after the Eq. (17):

The a priori tests using the data of laboratory measurements show that scale-similarity models with Gaussian or box filters provide correlation typically as high as 80% between real and modeled stresses (see, overview in Meneveau and Katz, 2000). The significant part of this correlation can be attributed to non-ideality of the spatial filter and use of common information for computing both the real and modeled stresses (see, Liu et al., 1994). The discrete spatial filter used in this study has a smooth transfer function in spectral space, so it can be supposed that the scale-similarity part of Eq. (18) is mainly responsible for the influence of velocity fluctuations belonging to "subfilter" scales.

In Section 4.2.3 we introduced next clarification of high correlation between subfilter velocity and resolved velocity:

In the previous subsection the recovered "subfilter" part of velocity  $\mathbf{u}'' = \mathbf{u}^* - \bar{\mathbf{u}}$  and so the subfilter Lagrangian velocity  $\mathbf{u}''^{(p)}$  were highly correlated with the resolved velocity  $\bar{\mathbf{u}}$  in time and space. This is due to the specifics of spatial filter (Eq. 24) used for the recovering given by Eqs. (25, 26). This filter has a smooth transfer function in spectral space. The analogous effects of non-ideal filters in LES which lead to the high correlations between modelled and measured turbulent stresses were obtained and discussed earlier in (Liu et al., 1994) and (Meneveau and Katz, 2000), where the laboratory data of turbulent flows were studied.

Section 5.1.4 contains the description of the universal function used for correction of dissipation profile. New reference was added to the paper which contains the measurement data of similar nondimensional function. The text after Eq. (43) was modified as follows:

Previous LES studies of stable ABL (e.g., Beare et al., 2006) also give neglectfully small val-

ues of the transport terms in TKE balance. The experimental confirmation of the validity of Eq. (42) can be found in (Grachev et al., 2015), where the dissipation in stable ABL was estimated using the spectral analysis of longitudinal velocity in inertial range. In accordance with this paper:  $\tilde{\epsilon} \approx \phi_m$ , that is almost indistinguishable from Eq. (42) within the accuracy of the experimental data and the ambiguity of the method of dissipation evaluation.

Section 5.1.5 contains the results of the evaluation of diffusion coefficients. Here these coefficients are presented as dimensional values and are specific for the modelled flow. There are no available experimental data on the values of horizontal diffusivity in horizontally homogeneous stable ABL. At least, authors are not aware of such measurements.

**9)** *Use Figures instead of Pictures in the paper.*

It was corrected.

**10)** *General remark in connection to Figure 6. Figure 6 shows a negative footprint. It is hard to understand the physical meaning of the negative values. Could you include a paragraph discussion this aspect?*

Next explanation was included into first paragraph of Section 4.3:

The negative values of scalar flux footprint show what the vertical turbulent transport of the scalar emitted in the relevant area is basically directed from the upper levels down to the surface. For example the positive surface concentration flux in this area will lead to negative anomaly of the turbulent flux measured in the sensor position. This does not contradict the diffusion approximation of the turbulent mixing, because mean crosswind advection at the upper levels can produce the positive vertical concentration gradient to the right of near-surface wind.

**11)** *in several places, e.g. line 24 at the page 11, the Equation number is referred without "Eq." so that it is difficult to understand what those numbers are for.*

It was corrected.

Additional references were included into bibliography:

Grachev, A. A., Andreas, E. L., Fairall, C. W., Guest, P. S. and Persson, P. O. G.: Similarity theory based on the Dougherty–Ozmidov length scale. *Q.J.R. Meteorol. Soc.*, 141, 1845–1856, 2015.

Liu S., Meneveau C., Katz J.: On the properties of similarity subgrid-scale models as deduced from measurements in a turbulent jet. *J. Fluid Mech.* 275, 83–119, 1994.

Meneveau C. and Katz J.: Scale-invariance and turbulence models for large-eddy simulation. *Annu. Rev. Fluid Mech.*, 32, 1–32, 2000. Michalek W.R., J.G. M.Kuerten, J.C.H. Zeegers, R.Liew, J.Pozorski, B.J. Geurts: A hybridstochastic-deconvolution model for large-eddy simulation of particle-laden flow. *Physics of Fluids*, 25, 123302, 2013

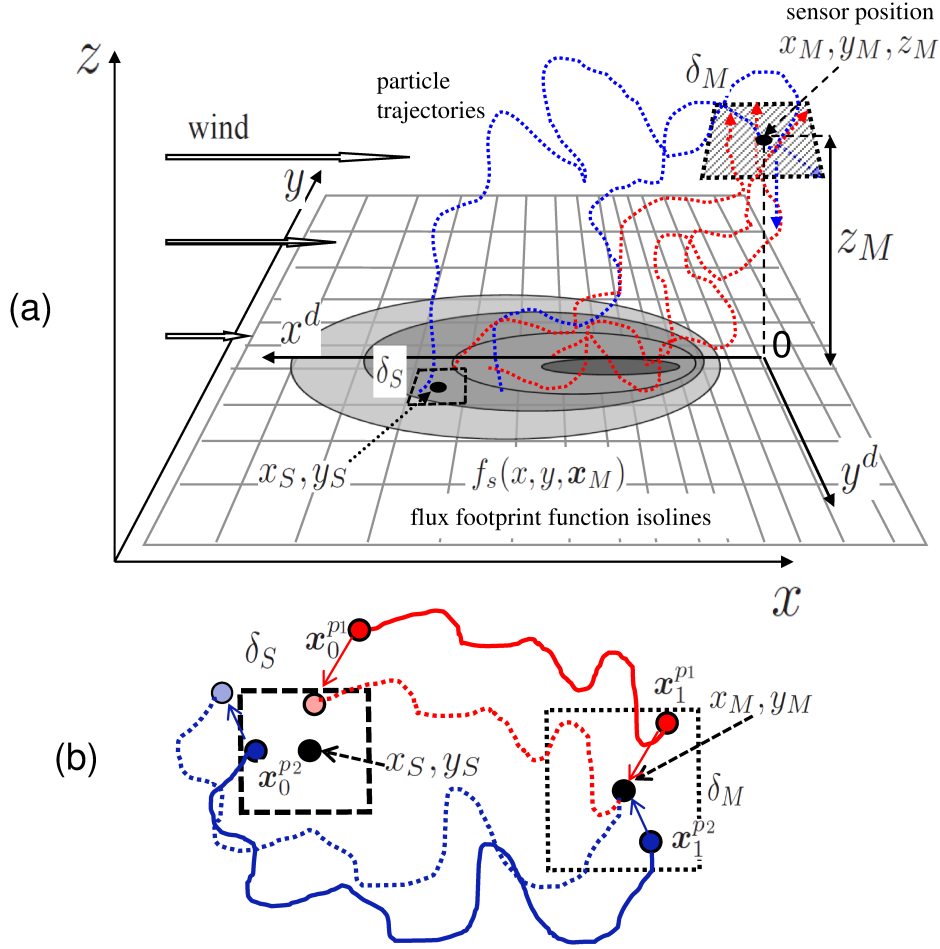


Figure 1: Schematic representation of footprint evaluation algorithm. (a) Setup of numerical experiment. (b) Example of two trajectories (red and blue bold curves). Shifted trajectories are shown by the dashed lines. Particle brings the impact into the value  $f_s(x_S, y_S, \mathbf{x}_M)$  if it intersects the test area  $\delta_M$  in vicinity of the sensor position  $\mathbf{x}_M$  and the origin of modified trajectory belongs to the test area  $\delta_S$ .